Design of High-Order Wideband Planar Balun Filter in S-Plane Bandpass Prototype

Yun-Wei Lin, Jhe-Ching Lu, and Chi-Yang Chang, *Member, IEEE*

***Abstract*—A new high-order wideband planar balun filter is proposed in this paper. The balun filter is exact synthesized based on S-domain bandpass prototype using Richards' Theorem to fit the user-defined specifications. By analyzing the redundant element in the equivalent circuit, the output impedance of the balun filter can be arbitrarily assigned. To use an S-plane bandpass prototype other than a high-pass prototype can shrink the circuit area and improve the stopband performance. The lumped capacitor approximation suppresses the spurious response in the stopband and further reduces the circuit size. A high-order balun filter with a bandwidth of 100% and a reflection coefficient of -15 dB is implemented by combining of microstrip lines, slotlines, and coplanar striplines. The simulation and measurement results match well.**

***Index Terms*—Balun filter, bandpass prototype, impedance transformation, planar structure, synthesis.**

I. Introduction

THE BALUN is an important component in microwave circuit design for transforming signals between unbalanced and balanced circuits [1]–[4]. In many applications of RF front-end modules, the balun is accompanied with a bandpass filter and matching network. To reduce the size of the circuit, the function of the filter, balun, and matching network can be combined, and the balun filter is then proposed [5]. Recently, there has been much literature written concerning the balun filters [6]–[8].

Among various balun structures [1]–[16], the Marchand balun is popular because it is easy to implement in planar form. Furthermore, it has a relatively wide bandwidth of amplitude and phase balance. The Marchand balun was proposed in 1944 [10], and it was later extended to fourth order by adding a unit element (UE) at both the balanced and unbalanced ports [11]. The circuit can be synthesized with a Chebyshev response by nonredundant synthesis [12], which is based on the S-plane high-pass prototype using Richards' transformation $S = j\tan(\pi/2(f/f_0))$, where f_0 is the center frequency of the passband.

Manuscript received August 16, 2011; revised February 28, 2012; accepted March 05, 2012. Date of publication May 01, 2012; date of current version June 26, 2012. This work was supported in part by the National Science Council under Grant NSC98-2221-E-009-034-MY3 and Grant NSC99-2221-E-009-050-MY3.

Y.-W. Lin and C.-Y. Chang are with the Department of Communication Engineering, National Chiao Tung University, Hsinchu 300, Taiwan (e-mail: weiga.cm96g@g2.nctu.edu.tw; mhchang@cc.nctu.edu.tw).

J.-C. Lu is with the RF Modeling Program, Taiwan Semiconductor Manufacture Company Ltd. (TSMC), Hsinchu 300, Taiwan (e-mail: Zill_gerching@hotmail.com).

Color versions of one or more of the figures in this paper are available online at http://ieeexplore.ieee.org.

Digital Object Identifier 10.1109/TMTT.2012.2193137

In [13], the planar coupled-line Marchand balun is also synthesized based on the S-plane high-pass prototype. However, the nonredundant synthesis lacks flexibility in bandwidth and impedance-transforming ratio, and it is constrained by the possibility of realizing extreme values of even- and odd-mode impedance of the coupled lines.

In [14], the authors synthesized a high-order Marchand balun and proposed a planar structure suitable for implementing the synthesized values. It performs a wideband response and flexible impedance transforming ratio. However, the spurious response occurs at a third of the center frequency due to the characteristic of the S-plane high-pass prototype. The poor upper stopband performance limits the filter application of the balun.

Recently, Fathelbab and Steer applied an S-plane bandpass prototype to synthesize many passive devices [15]–[17]. The Richards' transformation then becomes $S = j\tan(\pi/2(f/f_r))$, where f_r is the commensurate frequency at which all the stubs and transmission lines are a quarter-wavelength long. The spurious response can be designed higher than a third of the center frequency. Moreover, the circuit size can be further miniaturized by the lumped capacitors approximation. However, the working bandwidth is still constrained by the even- and odd-mode impedance values of coupled lines.

In this paper, we propose a wideband planar balun filter based on the S-plane bandpass prototype. The balun filter can be exactly synthesized. Section II analyzes the proposed balun and gives the equivalent two-port network form. Section III synthesizes the equivalent circuit. Section IV considers the impedance-transforming problem. Section V approximates the open-circuit stubs by the lumped capacitors, which further suppress the stopband spurious up to a fifth of the center frequency. Finally, some simulation and experimental results are presented.

II. Analysis of the Proposed Balun Filter

In theory, any order higher than two of the proposed balun filter could be synthesized. Here, a fifth-order balun filter is chosen as an example. The distributed circuit model of the proposed fifth-order balun filter is shown in Fig. 1(a), which consists of four open-circuit stubs, five short-circuit stubs and four interconnecting uniform transmission lines. The two-port network form can be obtained by combining port 2 and port 3 in series connection, as shown in Fig. 1(b). All the stubs and uniform transmission lines are a quarter-wavelength long at a designate frequency. Using the well-known Richards' transformation defined as

$$S = j\Omega = j\tan\left(\frac{\pi f}{2f_r}\right) \tag{1}$$

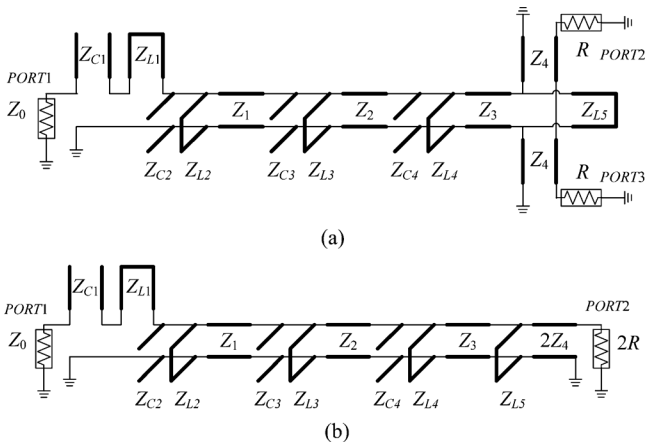

Fig. 1. (a) Structure of the proposed fifth-order balun filter. (b) Two-port network derived from the balun filter circuit in Fig. 1(a).

where Ω is the frequency variable in Richards' domain (S-domain), f is then the real frequency variable and f_r is the commensurate frequency at which all the stubs and transmission lines are a quarter-wavelength long. The S-domain equivalent circuit is shown in Fig. 2(a). It is a bandpass prototype in the S-plane, and obviously, there are redundant elements in the proposed network. However, the nonredundant prototype is needed for synthesizing the whole circuit. To simplify the circuit into nonredundant network, the Kuroda's identities, as shown in Fig. 2(b), are used.

Applying the Kuroda's identities to L_2 and Z_1, we get the transformed circuit in Fig. 2(c) with the following equation:

$$n = 1 + \frac{Z_1}{L_2}. \tag{2}$$

The transformer can then be absorbed by scaling the elements at the right-hand side of the transformer, as shown in Fig. 2(d). The equivalent circuit is shown in Fig. 2(e) with the following equation:

$$Z_1' = \frac{Z_1}{n} \quad Z_2' = \frac{Z_2}{n^2} \quad Z_3' = \frac{Z_3}{n^2} \quad Z_4' = \frac{2Z_4}{n^2} \tag{3}$$

$$L_3' = \frac{L_2 L_3}{n(nL_2 + L_3)} \quad L_4' = \frac{L_4}{n^2} \quad L_5' = \frac{L_5}{n^2} \tag{4}$$

$$C_3' = n^2 C_3 \quad C_4' = n^2 C_4 \quad R' = \frac{2R}{n^2}. \tag{5}$$

Following the previous procedure, we also apply the Kuroda's identities to L_3' and Z_2' with (6), and absorb the transformer to the right side. The transformed circuit is shown in Fig. 2(f). The values of the transformed elements Z_2'', Z_3'', Z_4'', C_4'', L_4'', L_5'', and R'' are obtained by scaling the element values in (3)–(5) with the variable n' as follows:

$$n' = 1 + \frac{Z_2'}{L_3'} \tag{6}$$

$$Z_2'' = \frac{Z_2'}{n'} \quad Z_3'' = \frac{Z_3'}{n'^2} \quad Z_4'' = \frac{Z_4'}{n'^2} \tag{7}$$

$$L_4'' = \frac{L_3' L_4'}{n'(n' L_3' + L_4')} \quad L_5'' = \frac{L_5'}{n'^2} \tag{8}$$

$$C_4'' = n'^2 C_4' \quad R'' = \frac{R'}{n'^2} \tag{9}$$

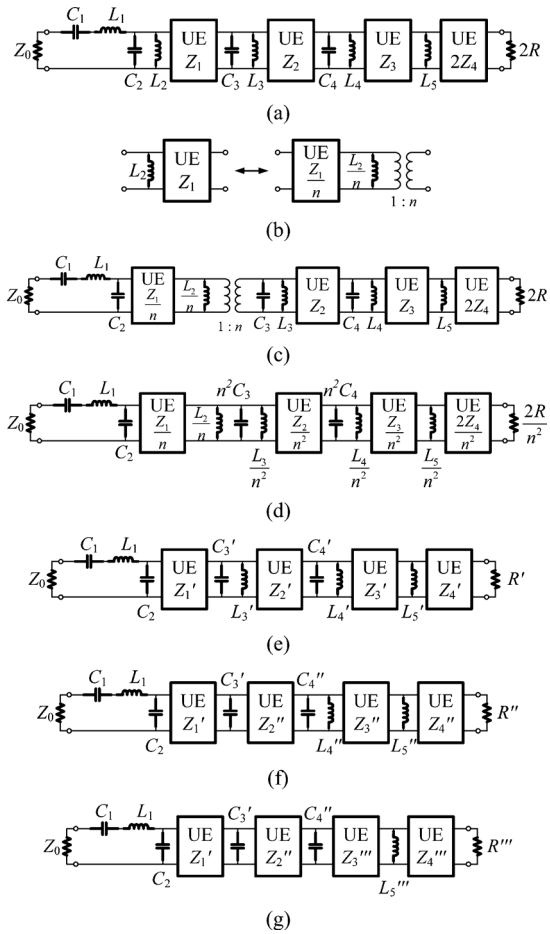

Fig. 2. (a) S-plane equivalent circuit of Fig. 1(b). (b)–(g) Procedure of circuit transformations to the nonredundant fifth-order S-plane bandpass prototype.

finally applying the Kuroda's identities to L_4'' and Z_3'' with (10) and absorbing the transformer again, we obtain the nonredundant S-plane bandpass prototype, as shown in Fig. 2(g). The transformed elements Z_3''', Z_4''', L_5''', and R''' are obtained by scaling the elements in the previous step with the variable n'' as follows:

$$n'' = 1 + \frac{Z_3''}{L_4''} \tag{10}$$

$$Z_3''' = \frac{Z_3''}{n''} \quad Z_4''' = \frac{Z_4''}{n''^2} \tag{11}$$

$$L_5''' = \frac{L_4'' L_5''}{n''(n'' L_4'' + L_4'')} \tag{12}$$

$$R''' = \frac{R''}{n''^2}. \tag{13}$$

Once the nonredundant S-plane bandpass prototype is achieved, a classical synthesis technique can be utilized to get the ideal element values [18]–[20].

III. Synthesis of S-Plane Bandpass Prototype

A. Synthesis Procedure

The classical synthesis technique is well documented in much of the literature [18]–[20]. By mapping the S-plane to the Z-plane with the following equation, the polynomial of

the Chebyshev response of the bandpass prototype can be calculated easily:

$$Z = \sqrt{\frac{S^2 - S_2^2}{S^2 - S_1^2}} \tag{14}$$

where S_1 and S_2 are the band-edge frequencies of the bandpass filter, which can be decided by (1). The next step is to form the following polynomial:

$$E(Z) + ZF(Z) = \prod_{i=1}^{N} (Z + Z_i) \tag{15}$$

where $E(Z)$ and $F(Z)$ are even polynomials in Z, and N is the number of transmission zeros, which is also the number of nonredundant elements in the network. Z_i is the value of the transmission zero that is corresponding to the transmission zero in the S-plane. For the low- and high-pass element in the S-plane, the transmission zeros are at ∞ and 0, respectively. For the UE, the transmission zero is at $\pm j$. Using (14), Z_i can then be calculated. The square of the magnitude characteristic function is then given by

$$|K(Z)|^2 = \frac{E^2(Z)}{E^2(Z) - O^2(Z)} \tag{16}$$

where the even function $E(Z)$ and odd function $O(Z)$, which is $ZF(Z)$, are calculated in (15). Transforming the characteristic function back to the S-plane $K(S)$ by (14), the square of the magnitude of the reflection transfer function can be derived from

$$|S_{11}(S)|^2 = \frac{\varepsilon^2 |K(S)|^2}{1 + \varepsilon^2 |K(S)|^2} = S_{11}(S) \cdot S_{11}(-S) \tag{17}$$

where ε is the equal-ripple value in the passband. The normalized input impedance of the network is given by

$$Z_{\text{in}}(S) = \frac{1 + S_{11}(S)}{1 - S_{11}(S)}. \tag{18}$$

Finally, using the pole-removing technique [21]–[24] and the Richards' theorem [25], all the values of L and C and the UE of the bandpass prototype can be synthesized.

B. Design Example

The fifth-order nonredundant bandpass prototype is given in Fig. 2(g). The resonant frequency f_r is set to be 2.5 GHz, the center frequency f_0 is 1 GHz, and the bandwidth is 100%, which leads f_1 and f_2 to be 0.5 and 1.5 GHz. Substituting f_1 and f_2 into (1), S_1 and S_2 are given as $j0.3249$ and $j1.3764$. ε is calculated to be 0.1807 for the passband return level of -15 dB.

There are four low-pass elements (series L or shunt C), two high-pass elements (series C or shunt L) and four UEs in Fig. 2(g). Substituting the four zeros at ∞, two zeros at 0, and four zeros at $\pm j$ into (14) and (15), we get the following polynomial shown in (19):

$$\begin{aligned} E(Z) + ZF(Z) = {} & Z^{10} + 18.94427191Z^9 + 154.2623792Z^8 \\ & + 713.7708764Z^7 + 2088.625711Z^6 \\ & + 4057.113656Z^5 + 5318.302859Z^4 \\ & + 4659.982833Z^3 + 2618.717801Z^2 \\ & + 854.0889837Z + 122.9918695. \end{aligned} \tag{19}$$

Using the even and odd polynomial in (19), the square of the magnitude characteristic function can be calculated by (16). Transforming back to the S-plane and using (17) and (18), the input impedance of the network in Fig. 2(g) with source impedance normalized to 1-Ω is then (20), shown at the bottom of this page. Applying the pole-removing technique and Richards' theorem, the value of each circuit element in Fig. 2(g) with normalized source impedance of 1- Ω can then be obtained as

$$\begin{aligned} Z_1' &= 1.1759 \quad Z_2'' = 0.4354 \\ Z_3''' &= 0.1486 \quad Z_4''' = 0.0442 \\ C_1 &= 2.0016 \quad C_2 = 1.2894 \\ C_3' &= 3.6346 \quad C_4'' = 9.0298 \\ L_1 &= 1.1724 \quad L_5''' = 0.1465 \quad R''' = 0.0949. \end{aligned} \tag{21}$$

The synthesized response is shown in Fig. 3. The response exactly matches the specification in the passband. Due to the characteristic of the Richards' transformation, the spurious response is periodical in the upper stopband.

IV. Impedance Transforming

The S-plane nonredundant bandpass prototype is synthesized in (21). It should be point out that, while simplifying the proposed redundant circuit in Fig. 2(a) to the nonredundant circuit in Fig. 2(g), there are three redundant inductors combined into the inductors L_3', L_4'', and L_5'''. Thus, there are three variables that can be decided by the designer when substituting the synthesized element values back into (2)–(13). Thus, the output port impedance R of the proposed balun filter can be specified arbitrarily, and all the impedances in Fig. 1(b) can be calculated exactly.

For example, if R in Fig. 1(a) is assigned to be equal to the source port impedance Z_0, the output load impedance $2R$ in Fig. 2(a) with a normalized source impedance of 1-Ω would be

$$Z_{\text{in}} = \frac{S^{10} + 0.85298S^9 + 4.7525S^8 + 3.126S^7 + 7.3515S^6 + 3.3298S^5 + 4.1782S^4 + 1.075S^3 + 0.78547S^2 + 0.080714S + 0.040325}{0.85298S^9 + 0.72757S^8 + 3.126S^7 + 1.8751S^6 + 3.3298S^5 + 1.1924S^4 + 1.075S^3 + 0.16155S^2 + 0.080714S} \tag{20}$$

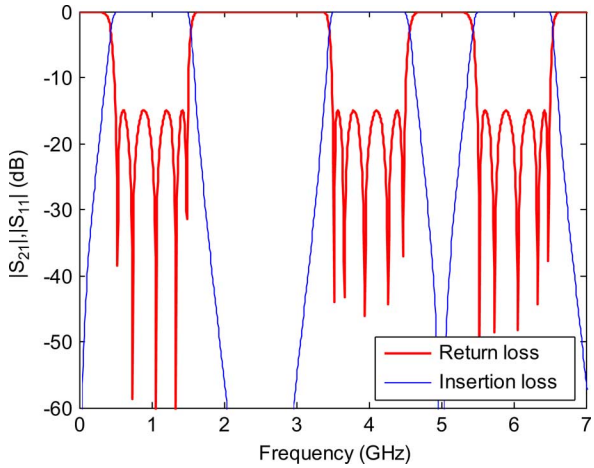

Fig. 3. Frequency response of the synthesized fifth-order bandpass prototype.

TABLE I
THEORETICAL CIRCUIT PARAMETERS OF BALUN FILTER

Specification	Return loss = 15dB BW = 100%	
$Z_{L1} = 58.618\,\Omega$	$Z_{C1} = 24.981\,\Omega$	$Z_1 = 79.451\,\Omega$
$Z_{L2} = 226.187\,\Omega$	$Z_{C2} = 38.777\,\Omega$	$Z_2 = 67.171\,\Omega$
$Z_{L3} = 142.848\,\Omega$	$Z_{C3} = 25.119\,\Omega$	$Z_3 = 77.906\,\Omega$
$Z_{L4} = 145.222\,\Omega$	$Z_{C4} = 28.877\,\Omega$	$Z_4 = 23.281\,\Omega$
$Z_{L5} = 31989\,\Omega$ (can be omitted)		

2. There are then still two scaling factors n' and n'' that can scale the impedances of the circuit to reasonable values that can be controlled by designer. Here, n' and n'' are set to be 1.69 and 2.01, respectively. Table I gives the theoretical impedance values of the proposed balun filter shown in Fig. 1(a) in a 50-Ω system.

V. PHYSICAL IMPLEMENTATION AND RESULTS

The impedance values of the proposed balun filter in Fig. 1(a) are synthesized as listed Table I. However, it is difficult to implement the series or parallel open- and short-circuit stub pair in the planar circuit. To simply the circuit, the lumped-element approximation is applied. As described in [15], because we use the S-plane bandpass prototype, the open-circuit stubs can be approximated by the lumped capacitors through the following equation:

$$j\left(\frac{1}{Z_{Ci}}\right)\tan\left(\frac{\pi f_0}{2f_r}\right) = j2\pi f_0 C_i \tag{22}$$

where Z_{Ci} is the synthesized ideal impedance value in Table I, and C_i is the approximated capacitor value. The above equation only approximates the characteristic of the open-circuit stubs at the vicinity of the designate center frequency. However, at the center frequency of each spurious passband, the value of each lumped capacitor will not fit the relation in (22). Using the advantage of this property, all the open-circuit stubs are substituted with lumped capacitors. The spurious response in the upper stopband in Fig. 3 can then be suppressed well. The calculated capacitor values are

$$\begin{aligned} C1 &= 6.3712\ \text{pF} \\ C2 &= 4.1044\ \text{pF} \\ C3 &= 6.3362\ \text{pF} \\ C4 &= 5.5116\ \text{pF} \end{aligned} \tag{23}$$

and the final equivalent circuit of the balun filter is shown in Fig. 4(a). The Z_{L5} section is omitted because the impedance synthesized in Table I is much larger than the intrinsic impedance in free space, which is equal to 377 Ω. The synthesized results are shown in Fig. 4(b) and (c).

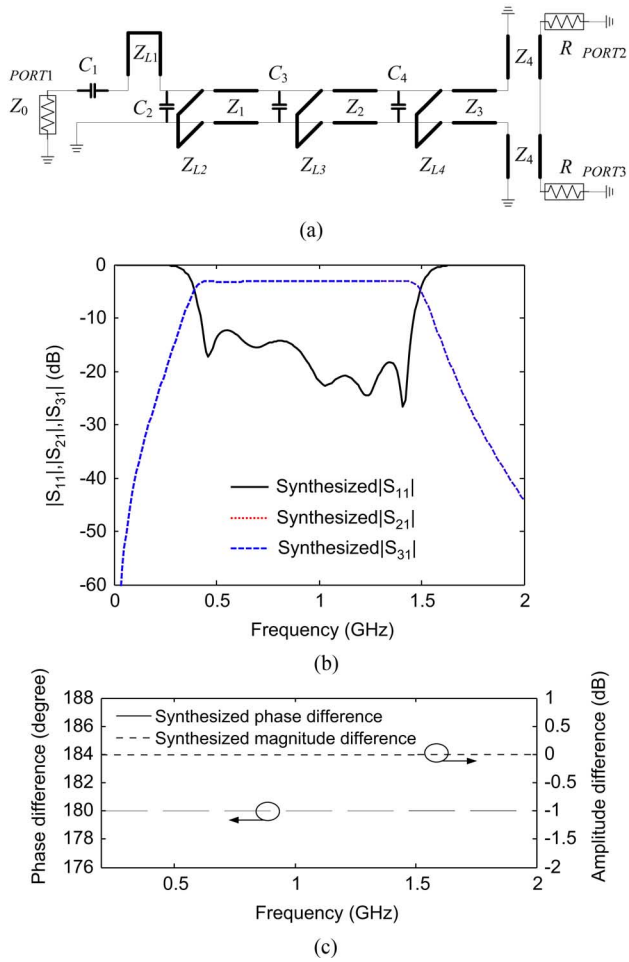

Fig. 4. (a) Final equivalent circuit of the balun filter. (b) Synthesized response. (c) Synthesized amplitude imbalance and phase difference of the balun filter.

The balun filter is implemented on an RT/Duroid 6010 board with a dielectric constant of 10.2 and a thickness of 0.635 mm (25 mil). The specification is given in the design example in Section III. Fig. 5 shows the schematic layout of the balun filter in Fig. 4(a). The physical dimensions are shown in Table II. The short-circuit stub Z_{L1}, UE Z_4, and the 50-Ω de-embedded section are implemented by microstrip lines. The short-circuit stub Z_{L2} and UE Z_2 are formed by coplanar striplines. To implement the whole circuit easily, the UE Z_1 and Z_3 use one section of coplanar stripline and one section of slotline. The short-circuit stubs Z_{L3} and Z_{L4} are implemented by offset microstrip lines,

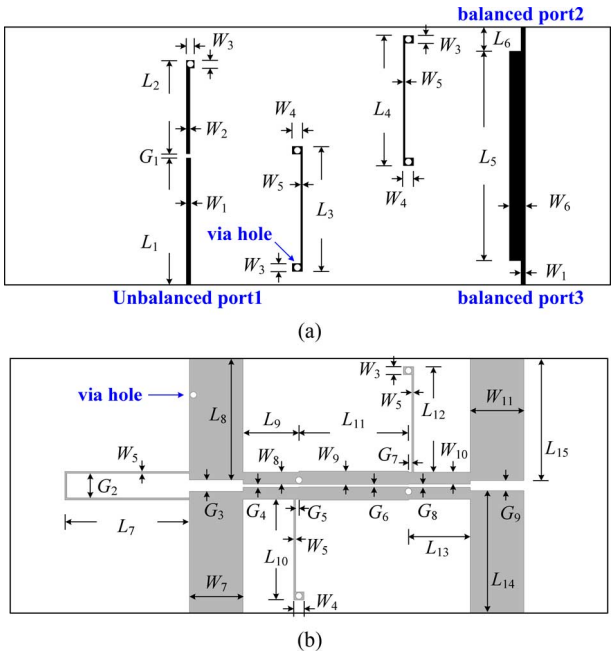

Fig. 5. Layouts show: (a) top and (b) bottom layers of the proposed balun filter.

TABLE II
PHYSICAL DIMENSIONS OF THE PROPOSED BALUN FILTER

The dimension of the balun filter corresponding to Fig. 5 (unit: mm)						
W1	*W2*	*W3*	*W4*	*W5*	*W6*	*W7*
0.584	0.483	1.016	1.321	0.254	2.057	6.858
W8	*W9*	*W10*	*W11*	*G1*	*G2*	*G3*
1.524	1.676	1.524	6.858	0.508	3.124	1.448
G4	*G5*	*G6*	*G7*	*G8*	*G9*	*L1*
0.406	0.406	0.330	0.406	0.406	1.295	15.977
L2	*L3*	*L4*	*L5*	*L6*	*L7*	*L8*
11.811	15.773	16.434	25.756	3.023	15.875	15.494
L9	*L10*	*L11*	*L12*	*L13*	*L14*	*L15*
7.112	12.827	13.970	13.462	7.874	15.596	15.570

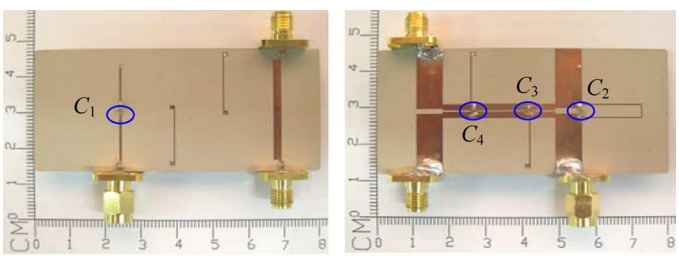

Fig. 6. (a) Top and (b) bottom views of the fabricated balun filter.

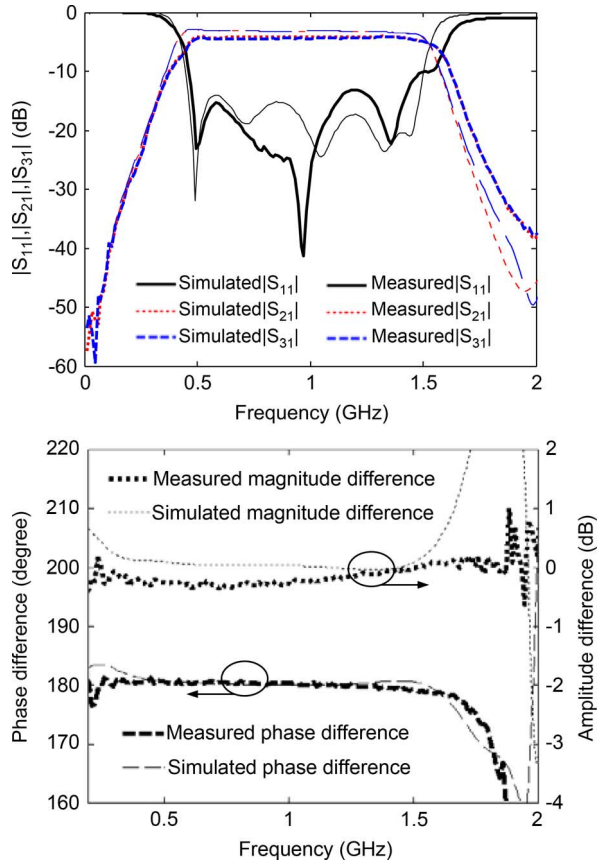

Fig. 7. Simulated and measured return loss, insertion loss, amplitude imbalance, and phase difference of the balun filter.

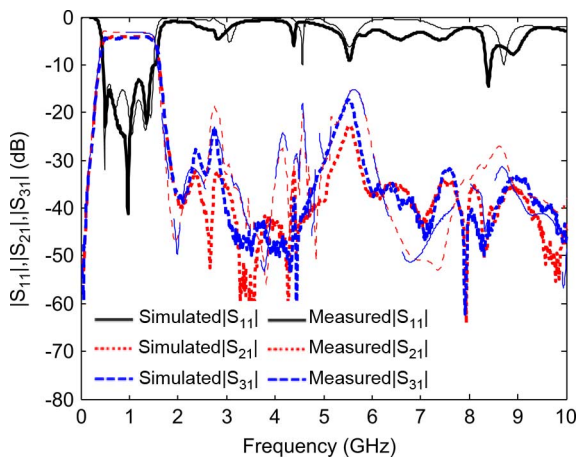

Fig. 8. Simulated and measured wideband response of the balun filter.

which are used to increase the characteristic impedance of the transmission lines. The commercial electromagnetic simulator HFSS is used to simulate and get the dimension of each transmission-line element. Combining all the transmission-line elements, as shown in Fig. 5, and adding internal ports at the places where the lumped capacitors should be soldered, the simulated result is then extracted into the circuit simulator ADS and optimized with the lumped capacitor values. Finally, the lumped capacitors C_1–C_4 are chosen to be 4.4, 2.5, 4.4, and 4 pF, respectively. The top and bottom view of the fabricated circuit is shown in Fig. 6. The capacitor C_1 is on the top layer, and the capacitors C_2–C_4 are on the bottom layer. The simulated and measured results are shown in Fig. 7. The return loss is almost under 15 dB in the passband, as we expected. The measured minimum insertion loss in the passband is $(3 + 1.07)$ dB, and the simulated minimum insertion loss is $(3 + 0.147)$ dB. The phase difference is within $180^\circ \pm 2^\circ$ in the passband, and the amplitude difference is within ± 0.4 dB in the passband. The measured responses match well with the simulated results.

TABLE III
COMPARISONS AMONG THE PUBLISHED AND PROPOSED BALUN FILTER

	Minimum Insertion Losses	Measured 3dB Bandwidths	Phase Balance	Amplitude Balance	Stopband Suppressions
[6]	3.4dB	3.5%	5°	1.1dB	30dB rejection up to about $1.5f_0$
[7]	1.43dB	10.9%	0.8°	0.2dB	30dB rejection up to about $2.5f_0$
[8]	1.45dB	5.8%	5°	0.5dB	N. A.
This work	1.07dB	112%	2°	0.4dB	23dB rejection up to about $5.2f_0$

Fig. 8 shows the wideband response of the proposed balun filter. It is obvious that the spurious of the theoretical response in Fig. 3 is periodically at 4, 6, and 9 GHz. Since all the open-circuit stubs are substituted by the lumped capacitors using (22), and it only approximates well at the designate center frequency of 1 GHz, the measured response shows better stopband rejection than the theoretical response. The upper stopband insertion loss is better than 23 dB up to 5.25 GHz, which is five times the center frequency. Table III compares the measured minimum insertion loss, 3-dB bandwidths, phase balance, amplitude balance, and the stopband suppressions for the published and proposed balun filter.

VI. CONCLUSION

A new wideband planar balun filter and its equivalent circuit model have been proposed. The exact synthesis method based on an S-plane bandpass prototype is used to calculate the circuit element values. By introducing the redundant elements, the impedance transforming balun filter could be easily obtained and the synthesized impedance value of each transmission-line section is suitable for practical implementation. Applying the lumped capacitors to substitute open-circuit stubs can suppress the spurious response of the filter in the upper stopband. A fifth-order balun filter has been implemented to verify the feasibility of the proposed filter.

REFERENCES

[1] S. C. Tseng, C. C. Meng, C. H. Chang, C. K. Wu, and G. W. Huang, "Monolithic broadband gilbert micromixer with an integrated Marchand balun using standard silicon IC process," *IEEE Trans. Microw. Theory Tech.*, vol. 54, no. 12, pp. 4362–4371, Dec. 2006.

[2] C. S. Lin, P. S. Wu, M. C. Yeh, J. S. Fu, H. Y. Chang, K. Y. Lin, and H. Wang, "Analysis of multiconductor coupled-line Marchand baluns for miniature MMIC design," *IEEE Trans. Microw. Theory Tech.*, vol. 55, no. 6, pp. 1190–1199, Jun. 2007.

[3] M. Chongcheawchamnan, K. S. Ang, J. N. H. Wong, and I. D. Robertson, "A push–pull power amplifier using novel impedance-transforming baluns," in *Proc. 30th Eur. Microw. Conf.*, Oct. 2000, pp. 1–4.

[4] H. K. Chiou and T. Y. Yang, "Low-loss and broadband asymmetric broadside-coupled balun for mixer design in 0.18-μm CMOS technology," *IEEE Trans. Microw. Theory Tech.*, vol. 56, no. 4, pp. 835–848, Apr. 2008.

[5] L. K. Yeung and K. L. Wu, "An LTCC balanced-to-unbalanced extracted-pole bandpass filter with complex load," *IEEE Trans. Microw. Theory Tech.*, vol. 54, no. 4, pp. 1512–1518, Apr. 2006.

[6] P. cheong, T. H. Lv, W. W. Choi, and K. W. Tam, "A compact microstrip square-loop dual-mode balun-bandpass filter with simultaneous spurious response suppression and differential performance improvement," *IEEE Microw. Wireless Compon. Lett.*, vol. 21, no. 2, pp. 77–79, Feb. 2011.

[7] T. Yang, M. Tamura, and T. Itoh, "Compact hybrid resonator with series and shunt resonances used in miniaturized filters and balun filters," *IEEE Trans. Microw. Theory Tech.*, vol. 58, no. 2, pp. 390–402, Feb. 2010.

[8] S. Sun and W. Menzel, "Novel dual-mode balun bandpass filters using single cross-slotted patch resonator," *IEEE Microw. Wireless Compon. Lett.*, vol. 21, no. 8, pp. 415–417, Aug. 2011.

[9] D. Kuylenstierna and P. Linner, "Design of broadband lumped-element baluns with inherent impedance transformation," *IEEE Trans. Microw. Theory Tech.*, vol. 52, no. 12, pp. 2739–2745, Dec. 2004.

[10] N. Marchand, "Transmission line conversion transformers," *Electron*, vol. 17, no. 12, pp. 142–145, Dec. 1944.

[11] J. Cloete, "Exact design of the Marchand balun," in *Proc. 9th Eur. Microw. Conf.*, Sep. 1979, pp. 480–484.

[12] M. C. Horton and R. J. Wenzel, "General theory and design of optimum quarter-wave TEM filters," *IEEE Trans. Microw. Theory Tech.*, vol. MTT-13, no. 3, pp. 316–327, May 1965.

[13] C. L. Goldsmith, A. Kikel, and N. L. Wilkens, "Synthesis of Marchand baluns using multilayer microstrip structures," *Int. J. Microw. Millimeter-Wave Comput.-Aided Eng.*, vol. 2, no. 3, pp. 179–188, 1992.

[14] J.-C. Lu, C.-C. Lin, and C.-Y. Chang, "Exact synthesis and implementation of new high-order wideband Marchand balun," *IEEE Trans. Microw. Theory Tech.*, vol. 59, no. 1, pp. 80–86, Jan. 2011.

[15] W. M. Fathelbab and M. B. Steer, "New classes of miniaturized planar marchand baluns," *IEEE Trans. Microw. Theory Tech.*, vol. 53, no. 4, pp. 1211–1220, Apr. 2005.

[16] W. M. Fathelbab and M. B. Steer, "Tapped Marchand baluns for matching applications," *IEEE Trans. Microw. Theory Tech.*, vol. 54, no. 6, pp. 2543–2551, Jun. 2006.

[17] W. M. Fathelbab, "The synthesis of a class of branch-line directional couplers," *IEEE Trans. Microw. Theory Tech.*, vol. 56, no. 8, pp. 1985–1994, Aug. 2008.

[18] H. J. Orchard and G. C. Temes, "Filter design using transformed variable," *IEEE Trans. Circuit Theory*, vol. CT-15, no. 4, pp. 385–408, Dec. 1968.

[19] R. J. Wenzel, "Synthesis of combline and capacitively loaded interdigital bandpass filters of arbitrary bandwidth," *IEEE Trans. Microw. Theory Tech.*, vol. MTT-19, pp. 678–686, Aug. 1971.

[20] J. A. G. Malherbe, *Microwave Transmission Line Filters*. Norwell, MA: Artech House, 1979.

[21] W. M. Max, *Microwave and RF Circuits: Analysis, Synthesis and Design*. Boston, MA: Artech House, 1992.

[22] L. Weinberg, *Network Analysis and Synthesis*. New York: McGraw-Hill, 1962.

[23] E. A. Guillemin, *Synthesis of Passive Networks*. New York: Wiley, 1957.

[24] N. Balabanian, *Network Synthesis*. Englewood Cliffs, NJ: Prentice-Hall, 1958.

[25] P. I. Richards, "General impedance-function theory," *Quart. Appl. Math*, vol. 6, pp. 21–29, 1948.

Yun-Wei Lin was born in Taipei, Taiwan, on May 3, 1985. He received the B.S. degree in communication engineering from National Chiao Tung University, Hsinchu, Taiwan, in 2007, and is currently working toward the Ph.D. degree in communication engineering at National Chiao-Tung University.

His research interests include the design and analysis of microwave circuits.

Jhe-Ching Lu was born in Kaohsiung, Taiwan, on May 18, 1982. He received the B.S. degree in electrical engineering from National Sun Yat-Sen University, Kaohsiung, Taiwan, in 2004, and the M.S. and Ph.D. degrees in communication engineering from National Chiao-Tung University, Hsinchu, Taiwan, in 2006 and 2009, respectively.

In 2009, he joined the Taiwan Semiconductor Manufacture Company Ltd. (TSMC), Hsinchu, Taiwan. He is currently with the RF Modeling Program, TSMC. His research interests include the analysis and design of microwave and millimeter-wave circuits and RF device characterization and modeling.

Chi-Yang Chang (S'88–M'95) was born in Taipei, Taiwan, on December 20, 1954. He received the B.S. degree in physics and M.S. degree in electrical engineering from the National Taiwan University, Taipei, Taiwan, in 1977 and 1982, respectively, and the Ph.D. degree in electrical engineering from The University of Texas at Austin, in 1990.

From 1979 to 1980, he was with the Department of Physics, National Taiwan University, as a Teaching Assistant. From 1982 to 1988, he was with the Chung-Shan Institute of Science and Technology (CSIST), as an Associate Researcher, where he was in charge of development of microwave integrated circuits (MICs), microwave subsystems, and millimeter-wave waveguide E-plane circuits. In 1990, he returned to CSIST, where until 1995, he was an Associate Researcher in charge of development of uniplanar circuits, ultra-broadband circuits, and millimeter-wave planar circuits. In 1995, he joined the faculty of the Department of Electrical Engineering, National Chiao-Tung University, Hsinchu, Taiwan, as an Associate Professor and became a Professor in 2002. His research interests include microwave and millimeter-wave passive and active circuit design, planar miniaturized filter design, and monolithic-microwave integrated-circuit (MMIC) design.